Science Press

ARTICLE

Fabrication of ZrB₂-based Ultra-high Temperature Ceramics by SPS Using Nanosized ZrB₂ Powders

Gui Kaixuan[1],   Zhang Qingda[1],   Zhu Dongdong[2],   Wang Gang[1]

[1] *Anhui Polytechnic University, Wuhu 241000, China;* [2] *Key Laboratory of Air-Driven Equipment Technology of Zhejiang Province, Quzhou University, Quzhou 324000, China*

Abstract: The spark plasma sintering behaviors of ZrB_2-based ultra-high temperature ceramics were investigated using nanosized ZrB_2 powders. Results show that rapid densification occurs at low temperature (1550 °C) for monolithic ZrB_2 due to the nanosized powders. ZrB_2-SiC ceramics were fully densified by SPS at 1800 °C, thus obtaining a high flexural strength of 1078±162 MPa. ZrB_2-SiC-C_f composites are prepared by SPS at 1700 °C. The composites show obvious fiber pull-out on the fracture surface, leading to a high fracture toughness (6.04 MPa·m$^{1/2}$) and a non-brittle fracture mode. Meanwhile, a high critical thermal shock temperature difference of 627 °C is obtained for ZrB_2-SiC-C_f, implying excellent thermal shock resistance of such material.

Key words: ZrB_2; ultra-high temperature ceramics; spark plasma sintering; carbon fiber

Ultra-high temperature ceramics (UHTCs) have drawn increasing attention in recent years due to their unique combination of properties, such as high melting point, high strength, high electrical and thermal conductivity and excellent oxidation resistance [1-5]. ZrB_2 is a very attractive candidate for aerospace applications under extreme environments due to its outstanding high temperature properties as well as lower density compared to other UHTCs [6,7]. However, one of the greatest obstacles to the successful development and implementation of ZrB_2-based UHTCs is their inherent brittleness (such as low fracture toughness and poor thermal shock resistance), which can lead to catastrophic damage of such materials [8]. The introduction of carbon fibers is an effective approach to toughen ZrB_2-based UHTCs via some toughen mechanisms such as fiber pull out, fiber bridging and crack deflecting [9-12]. Due to strong covalent bonding and low self-diffusion coefficients, typical dense ZrB_2-based UHTCs require high sintering temperatures [13]. However, fiber degradation caused by the reaction between carbon fiber and ceramic compositions at high sintering temperature will significantly

weaken the toughening effects of carbon fibers [14-16]. Therefore, it is necessary to enhance densification and to reduce the sintering temperature of ZrB_2-based UHTCs to inhibit the fiber degradation.

Research has shown that the addition of SiC (20 vol%~30 vol%) can lower the densification temperature, improve mechanical properties and remarkably increase the oxidation resistance of ZrB_2 [17-19]. Another strategy typically adopted to lower the sintering temperature and to enhance sinterability of ZrB_2 is to use nanosized powders instead of micronsized ones as starting materials since the sintering temperature of nanosized particles is dramatically lower than that of micronsized counterparts [20,21]. It is well known that spark plasma sintering (SPS) demonstrate many benefits for the densification of nanoceramics, and one of the most remarkable features of SPS is the small grain size the process can maintain while achieving full densification [22-24]. Zamora et al[21] explored the feasibility of reducing the SPS temperature of additive-free ZrB_2 ceramics via crystal size refinement of the starting powder down to the low nanoscale, and the results revealed that nanoscale ZrB_2 can be

densified at temperatures 250~450 °C, lower than that for the typical micrometer and submicrometre ZrB_2 powders. However, few literatures systematically reported the microstructures and properties of ZrB_2-based UHTCs fabricated by SPS, especially the carbon fiber toughened ZrB_2-based UHTCs.

The purpose of this research is to systematically investigate the SPS behaviors, microstructure evolution and properties of ZrB_2-based UHTCs (including ZrB_2, ZrB_2-SiC and ZrB_2-SiC-C_f composites) using nanosized ZrB_2 powders. The thermal shock resistance of ZrB_2-SiC-C_f composites fabricated by SPS was also reported.

1 Experiment

Commercial powders were used to prepare the ceramic composites: ZrB_2 powders (Beijing HWRK Chem Co., Ltd., China), average particle size 150 nm; SiC powders (Kaihua, China), average particle size 0.45 μm; carbon fibers (T800, Tokyo, Japan), average diameter 5 μm, average chopped length ~2 mm. For monolithic ZrB_2 fabricated by SPS, nanosized ZrB_2 powders were directly put into graphite die and sintered in SPS system (KCE®-FCT-HPD-250, Germany) at 1300, 1400, 1500, 1600, 1700 and 1800 °C under a pressure of 40 MPa for 10 min. For ZrB_2-SiC or ZrB_2-SiC-C_f composites, 20 vol% SiC or 20 vol% SiC plus 30 vol% C_f were added into ZrB_2 powders. The powder mixtures were dispersed in ethanol and ball milled in a Teflon-coated tank at 220 r/min for 8 h, using ZrO_2 balls as media. To minimize segregation by sedimentation during drying, the slurry was dried in a rotary evaporator at a temperature of 75 °C and a rotation speed of 40 r/min. The dried powders were sintered by SPS at different temperatures (1600, 1700, 1800 °C for ZrB_2-SiC, and 1700 °C for ZrB_2-SiC-C_f) under a pressure of 40 MPa for 10 min. The shrinkage curve of the sample was recorded by a dilatometer at a resolution of 0.005 mm.

The bulk density of sintered specimens was identified based on the Archimedean principle with deionized water as medium. The theoretical density of corresponding samples was calculated through rule of mixture. Flexural strength was tested in three-point bending on 3 mm×4 mm×36 mm bars, using a 30 mm span and a crosshead speed of 0.5 mm/min. Fracture toughness was evaluated using single-edge notched beam (SENB) on 2 mm×4 mm×22 mm bars with a 16 mm span and a crosshead speed of 0.05 mm/min. A minimum number of five specimens were tested for each experimental condition. The microstructure of each specimen was examined by scanning electron microscopy (SEM; S-570, Hitachi, Tokyo), transmission electron microscopy and high-resolution transmission electron microscopy (TEM and HR-TEM, Tecnai G^2-F30, USA). The preparation of the TEM sample was performed by focused ion beam (FIB, FEI 600i, USA). The thermal

shock behavior of ZrB_2-SiC and ZrB_2-SiC-C_f were evaluated by a water-quenching technique. The test samples (3 mm×4 mm×36 mm) were heated to the selected temperature (225~825 °C) in a furnace in air and maintained at that temperature for 10 min to eliminate the homogeneous temperature distribution. The samples were transferred from furnace to a water bath (25 °C) in a very short time (<0.5 s). At last, the residual strength of the samples after thermal shock was tested by three-point bending test. The critical thermal shock temperature difference ($\triangle T_c$) was defined as the temperature difference at which the materials remain 70% of the initial strength, which was determined using linear interpolation of the residual strength values [25].

2 Results and Discussion

2.1 Spark plasma sintering of ZrB_2

The relative density and the grain sizes of ZrB_2 fabricated by SPS at 1300~1800 °C are exhibited in Fig.1. The relative density of ZrB_2 increases slightly from 70.1% to 72.8% as the sintering temperature increases from 1300 °C to 1500 °C. The corresponding ZrB_2 grain sizes are in the range of 0.15~0.25 μm (almost equal to the starting ZrB_2 powder size), which indicates that the low sintering temperature does not lead to significant grain growth. Further improvement in the sintering temperature results in rapid densification of ZrB_2, and the relative density increases almost linearly from 82.3% at 1600 °C to 98.0% at 1800 °C. Guo et al [23] systematically investigated the densification behavior and grain growth of ZrB_2 ceramics fabricated by SPS using micronsized powders (1.5~2.5 μm) and a low relative density of ~88% was obtained at 1800 °C. Sciti et al [26] also demonstrated that the full densification temperature for micronsized ZrB_2 powders should be exceeding 2100 °C. These results imply that the densification behavior of ZrB_2 ceramics in the present work is remarkably enhanced by reducing the starting powder size. However, exaggerated grain growth occurs at 1600~1800 °C and most nanosized ZrB_2 powders are transformed into micrometer sized ZrB_2 grains (~2.12 μm at 1800 °C). On the one hand, the increased sintering temperature can provide sufficient driving force for grain growth during sintering. On the other hand, the increased relative density can decrease the diffusion distance for surface diffusion and grain boundary diffusion, which should be also responsible for the exaggerated grain growth of ZrB_2. The densification behavior of the nanosized ZrB_2 powders by SPS at 1800 °C for 10 min is monitored using the sintering temperature-time and displacement-time curves, as shown in Fig.2. Note that the rapid rise of the displacement below 800 °C is due to the applied pressure of 30 MPa. According to the measured displacement-time curve, the densification can be divided into three stages. The first stage: the displacement gradually increases as the sintering temperature increases from 800 °C up

to 1550 °C. The densification rate in the first stage is very slow. The second stage: rapid densification of the nanosized ZrB_2 powders occurs at the temperature range of 1550~1650 °C. In this stage, the temperature can provide enough driving force to promote mass transport and diffusion between the adjacent contacted particles in a large scale [27], resulting in a high densification rate. Due to the covalent bonding, low volume and grain boundary diffusion rates, typical onset temperature for rapid densification of micronsized ZrB_2 powders is above 1700 °C [2], significantly higher than the value of 1550 °C in this work. The third stage: the displacement begins to flatten and the densification rate gradually decreases to zero when the sample is densified at dwell temperature for 3.7 min.

The typical microstructures of fracture surfaces of ZrB_2 ceramics prepared by SPS at 1300~1800 °C are presented in Fig.3. The fracture surfaces are mainly intergranular for these ceramics. Denser microstructures and coarser grains are found in ZrB_2 at higher sintering temperatures, which is in accordance with the values of relative density and grain size shown in Fig.1. In addition, ZrB_2 ceramics fabricated by SPS at 1700 and 1800 °C display very clean grain boundaries without any other impurities located between the ZrB_2 grain boundaries, which is also found in other ceramics prepared by SPS [28].

Fig.3   SEM images of fracture surfaces of ZrB_2 prepared by SPS at different temperatures: (a) 1300 °C, (b) 1400 °C, (c) 1500 °C, (d) 1600 °C, (e) 1700 °C, and (f) 1800 °C
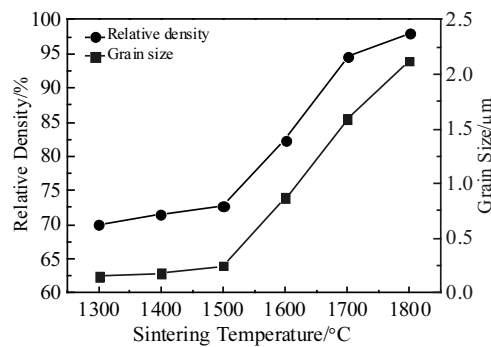

Fig.1   Relative density and grain size of ZrB_2 fabricated by SPS as a function of sintering temperature in the range of 1300~1800 °C
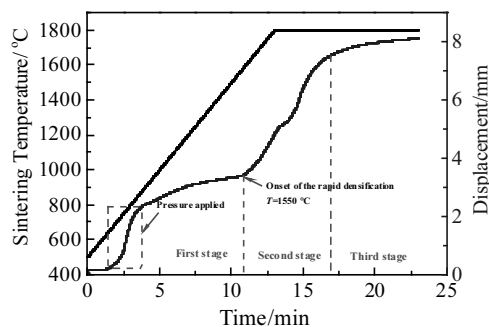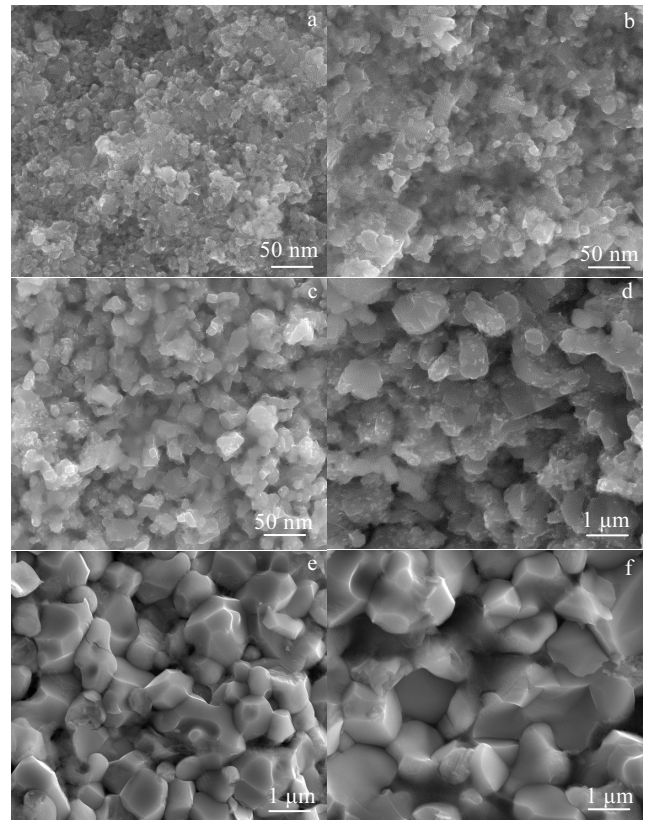

Fig.2   Densification behavior of nano-sized ZrB_2 powders in SPS process

2.2   Spark plasma sintering of ZrB_2-SiC

Research has shown that the addition of SiC helps to enhance the sinterability and improve the mechanical properties of ZrB_2 [13]. However, few literatures reported the sinterability of ZrB_2-SiC using nanosized ZrB_2 powders. In the present study, the densification behavior and grain growth of ZrB_2-SiC during SPS process were investigated. The relative density, average ZrB_2 grain sizes and flexural strengths of ZrB_2 and ZrB_2-SiC were compared (shown in Table 1). The relative density of ZrB_2-SiC fabricated by SPS at 1600~1800 °C was 93.5%~99.7%, obviously higher than that of ZrB_2 consolidated under the same SPS condition. It should be noted that the full densification temperature for ZrB_2-SiC is 1800 °C which is significantly lower than the reported values [13, 29]. The microstructures on the fracture surfaces of ZrB_2-SiC sintered at 1600~1800 °C are shown in Fig.4. The white phases are ZrB_2 matrix and the black contrasting ones are SiC secondary phases. The average grain sizes of ZrB_2 in ZrB_2-SiC are determined to be 0.72~1.89 μm, which are much smaller than those of monolithic ZrB_2 sintered under the same conditions. Indeed, the added SiC particulates can act as grain growth inhibitors which can reduce the grain boundary mobility or fix the

grain boundary, resulting in enhanced densification and re-fined ZrB_2 grain size [13]. The addition of SiC increases the flexural strength of ZrB_2 from 223~451 MPa to over 600 MPa, especially a high flexural strength of 1078 MPa for the nearly-dense ceramic sintered at 1800 °C. Research has shown that although the ZrB_2 grain size is an important factor affecting the flexural strength of ZrB_2-SiC ceramics, it is not a limiting factor. Comparing the strength values measured in ZrB_2-SiC sintered at different temperatures, it seems that the effect of the relative density on the strength is much greater than that of the ZrB_2 grain size.

Fig.5a shows the TEM image of ZrB_2-SiC fabricated by SPS at 1800 °C, and the corresponding element distribution on the observed area is shown in Fig.5b~5f. The main elements detected by EDS included Zr, B, Si and O. Carbon is not detected because SiC is not found in the observed area. Small amount of O exists in the form of ZrO_2 and SiO_2 (shown in position 1, position 2 and position 3 in Fig.5b) that are derived from the surface oxidation of the starting ZrB_2 and SiC powders, respectively. Additionally, some dislocations are clearly observed in the ZrB_2 grain (shown in Fig.5a) and the high magnification image reveals that these dislocations likely originate from the ZrB_2 grain boundary, as shown in Fig.6a, which are further confirmed by HR-TEM images exhibited in Fig.6b and 6c. These dislocations might derive from the residual stress generated at the ZrB_2 grain boundaries during the rapid cooling stage in SPS. However, most ZrB_2 grain boundaries appear to be

coherent boundaries as shown in Fig.6d, which might lead to a high flexural strength of such material.

2.3 Spark plasma sintering of ZrB_2-SiC-C_f

Research has shown that the addition of carbon fibers can substantially improve the toughness of ZrB_2-based ceramics, and it is important to promote densification and to inhibit the degradation of carbon fibers by appropriate methods in the fabrication of carbon fiber toughened ZrB_2 ceramic composites. Our previous work revealed that the fiber deg-radation can be effectively inhibited in ZrB_2-SiC-C_f com-posites by hot pressing (HP) at low temperature using nanosized ZrB_2 powders [8,16]. In order to confirm the effect of SPS process on the microstructure and performance of ZrB_2-SiC-C_f composite, ZrB_2-SiC composites containing 30 vol% carbon fibers are consolidated by SPS at 1700 °C for 10 min in the present study. The measured bulk density of ZrB_2-SiC-C_f is 4.12 g/cm^3 which corresponds to the relative density of 97.6%, slightly lower than that of ZrB_2-SiC fab-ricated under the same SPS conditions. This indicates that the addition of 30 vol% carbon fibers cannot impede the densification of ZrB_2-SiC-C_f owing to the uniform distribu-tion of the carbon fibers among the ZrB_2-SiC ceramic ma-trix, as shown in Fig.7a. The XRD pattern of ZrB_2-SiC-C_f is plotted in Fig.7b. It can be seen that only ZrB_2, SiC and a few ZrO_2 peaks are observed, and no carbon peaks are de-tected, implying that graphitization of carbon fibers does not occur during the SPS process [30]. ZrO_2 phase detected in ZrB_2-SiC-C_f is derived from the oxygen contamination on

Table 1   Relative density and flexural strength of ZrB_2 and ZrB_2-SiC fabricated by SPS at different temperatures

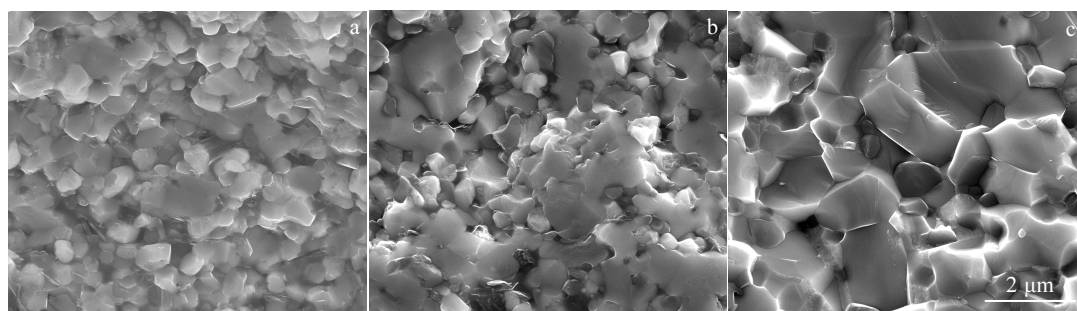| Materials	Sintering temperature/°C	Relative density/%	ZrB_2 grain size/μm	Flexural strength/MPa
ZrB_2	1300	70.1	0.15	-
ZrB_2	1400	71.4	0.18	-
ZrB_2	1500	72.8	0.25	-
ZrB_2	1600	82.3	0.87	223±40
ZrB_2	1700	94.6	1.59	301±43
ZrB_2	1800	98.0	2.12	451±52
ZrB_2-SiC	1600	93.5	0.72	605±71
ZrB_2-SiC	1700	98.8	1.23	835±126
ZrB_2-SiC	1800	99.7	1.89	1078±162

Fig.4   SEM images of fractured surfaces of ZrB_2-SiC prepared by SPS at 1600 °C (a), 1700 °C (b), and 1800 °C (c)
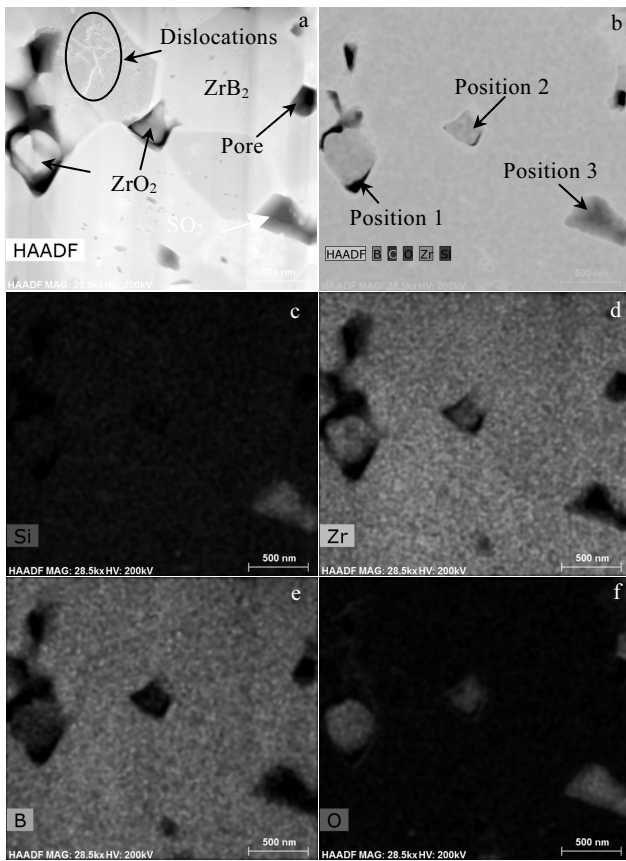
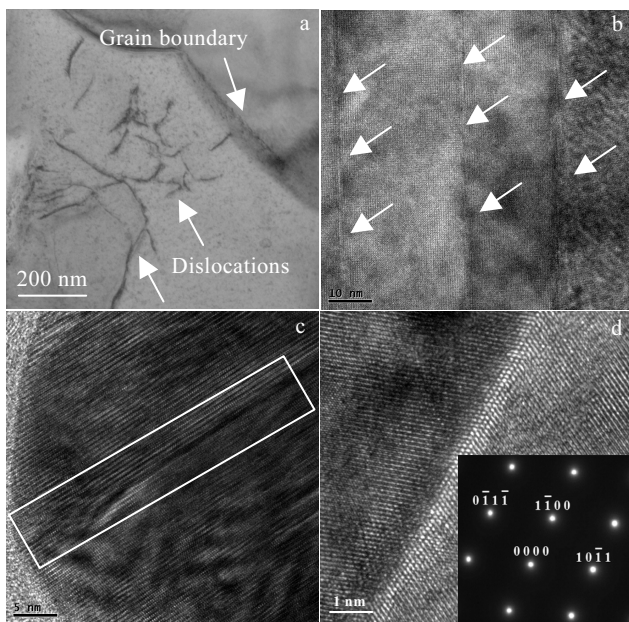Fig.5   TEM image (a) and the element distribution (b~f) of ZrB$_2$-SiC fabricated by SPS at 1800 °C

Fig.6   TEM image (a) of dislocations in the ZrB$_2$-SiC fabricated by SPS at 1800 °C; HR-TEM images of ZrB$_2$/ZrB$_2$ inter-face (b, c) and ZrB$_2$ grain boundaries (d)

the surface of the nanosized ZrB$_2$ starting powders. The measured fracture toughness of the ZrB$_2$-SiC-C$_f$ composite is 6.04 MPa·m$^{1/2}$, obviously higher than that of ZrB$_2$-SiC (5.68 MPa·m$^{1/2}$) fabricated under the same SPS process. Fiber pull-out can be easily observed on the fracture surface of the ZrB$_2$-SiC-C$_f$ composite, as shown in Fig.7c and 7d, which should be the main reason for the improvement of the fracture toughness. Our previous work showed that se-vere fiber degradation occurs in the ZrB$_2$-SiC-C$_f$ composite fabricated by SPS at 1900 °C for 10 min [16]. While, the carbon fiber almost retains its smooth surface after SPS at 1700 °C in the present work (Fig.7d). The results indicate that the fiber degradation can be effectively inhibited by decreasing the sintering temperature of the ZrB$_2$-SiC-C$_f$ composite.

Fig.8 shows the typical load-displacement curves re-corded during the SENB tests for ZrB$_2$-SiC-C$_f$ and ZrB$_2$-SiC fabricated by SPS at 1700 °C for 10 min. The fracture modes of these two materials are quite different. ZrB$_2$-SiC displays a typical brittle fracture mode during the SENB test. In case of ZrB$_2$-SiC-C$_f$, the load almost linearly increases to the maximum load and then gradually de-creases to a low value, which can be seen as a non-brittle fracture mode. The difference in fracture mode implies that the crack propagation of ZrB$_2$-SiC-C$_f$ is more stable than that of ZrB$_2$-SiC owing to the toughening mechanism such as fiber pull-out, crack deflecting and crack branching, which can avoid a catastrophic damage of such materials [31]. Moreover, the elasticity modulus (evaluated as the slope of the load-displacement curve before fracture in Fig.5) of ZrB$_2$-SiC-C$_f$ is obviously lower than that of ZrB$_2$-SiC, which is beneficial for improving the thermal shock resis-tance of the materials[32].
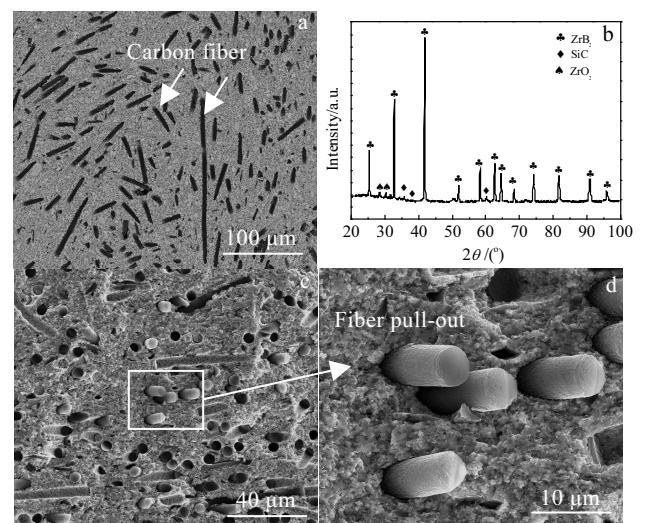

Fig.7   SEM images of polished surface (a) and fractured surface (c, d); XRD pattern (b) of ZrB$_2$-SiC-C$_f$ composites fabricated by SPS at 1700 °C for 10 min

The thermal shock resistance of ZrB_2-SiC-C_f and ZrB_2-SiC fabricated by SPS at 1700 °C for 10 min was evaluated by water-quenching method. The residual strength vs thermal shock temperature difference for two materials is plotted in Fig.9. The residual strength of ZrB_2-SiC remains at 817~835 MPa as the thermal shock temperature difference (ΔT) is below 300 °C, while it sharply decreases to 180 MPa when ΔT=400 °C and then gradually decreases with increasing the ΔT. The calculated critical thermal shock temperature difference (ΔT_c) is 336 °C for ZrB_2-SiC. In case of ZrB_2-SiC-C_f, the residual strength decreases very slowly from 412 MPa to 348 MPa as the ΔT increases from 0 °C to 600 °C, and then decreases to 124 MPa. The calculated ΔT_c of ZrB_2-SiC-C_f is 627 °C, almost twice larger than that of ZrB_2-SiC, which indicates that the incorporation of carbon fibers into ZrB_2-based ceramics can significantly improve the thermal shock resistance of such materials.
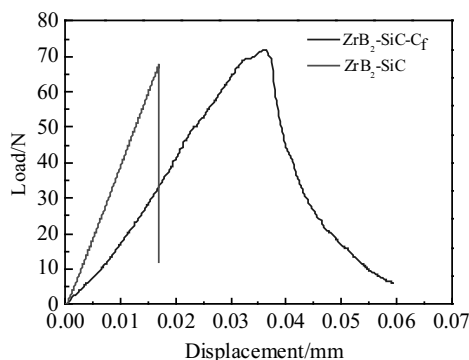

Fig.8   Typical load-displacement curves for ZrB_2-SiC-C_f composite and ZrB_2-SiC ceramics fabricated by SPS at 1700 °C for 10 min
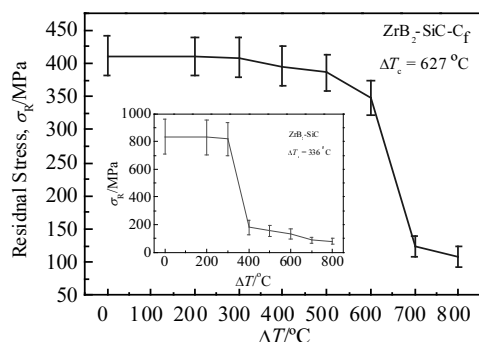

Fig.9   Residual strength vs thermal shock temperature difference for ZrB_2-SiC (inset) and ZrB_2-SiC-C_f composites

3   Conclusions

1) ZrB_2, ZrB_2-SiC and ZrB_2-SiC-C_f composite are consolidated by SPS at different temperatures using nanosized

ZrB_2 powders (150 nm). Low relative density (70.1%~72.8%) of monolithic ZrB_2 is obtained during SPS at 1300~1500 °C, and then increases almost linearly with increasing the sintering temperature at 1500~1800 °C.

2) The addition of SiC can significantly enhance the densification of ZrB_2 and full densification of ZrB_2-SiC is attained by SPS at 1800 °C. The average ZrB_2 grain size in ZrB_2-SiC ranges from 0.72 μm at 1600 °C to 1.89 μm at 1800 °C, smaller than that of monolithic ZrB_2 prepared under the same SPS condition. ZrB_2-SiC shows much higher flexural strength than monolithic ZrB_2 owing to its denser microstructure and finer grain.

3) The fracture toughness of ZrB_2-SiC fabricated by SPS at 1700 °C is improved from 5.68 to 6.04 MPa·m$^{1/2}$ with the addition of 30 vol% carbon fibers, and the ZrB_2-SiC-C_f composites show non-brittle fracture mode and excellent thermal shock resistance with a high critical thermal shock temperature difference of 627 °C, which is almost twice larger than that of ZrB_2-SiC.

References

1 Nisar A, Ariharan S, Balani K. *Ceramics International*[J], 2017, 43(16): 13 483

2 Guo S Q. *Journal of the European Ceramic Society*[J], 2009, 29(6): 995

3 Fahrenholtz W G, Hilmas G E, Talmy I G *et al*. *Journal of the American Ceramic Society*[J], 2007, 90(5): 1347

4 Simonenko E P, Sevast'yanov D V, Simonenko N P *et al*. *Russian Journal of Inorganic Chemistry*[J], 2013, 58(14): 1669

5 Fahrenholtz W G, Hilmas G E. *Scripta Materialia*[J], 2017, 129: 94

6 Chamberlain A L, Fahrenholtz W G, Hilmas G E *et al*. *Journal of the American Ceramic Society*[J], 2004, 87(6): 1170

7 Monteverde F, Guicciardi S, Bellosi A. *Materials Science and Engineering A*[J], 2003, 346(1-2): 310

8 Gui Kaixuan, Liu Fangyu, Wang Gang *et al*. *Journal of Advanced Ceramics*[J], 2018, 7(4): 343

9 Sha J J, Li J, Lv Z Z *et al*. *Journal of the European Ceramic Society*[J], 2017, 37(2): 549

10 Guo S. *Ceramics International*[J], 2013, 39(5): 5733

11 Silvestroni L, Dalle Fabbriche D, Melandri C *et al*. *Journal of the European Ceramic Society*[J], 2016, 36(1): 17

12 Xiao Kesong, Guo Quangui, Liu Zhanjun *et al*. *Ceramics International*[J], 2014, 40(1): 1539

13 Zhu S, Fahrenholtz W G, Hilmas G E. *Journal of the European Ceramic Society*[J], 2007, 27(4): 2077

14 Yang Feiyu, Zhang Xinghong, Han Jiecai *et al*. *Journal of Alloys and Compounds*[J], 2009, 472(1-2): 395

15 Yang Feiyu, Zhang Xinghong, Han Jiecai *et al*. *Materials Letters*[J], 2008, 62(17-18): 2925

16 Gui K, Hu P, Hong W *et al*. *Journal of Alloys and Compounds*[J], 2017, 706: 16

17 Liu Qiang, Han Wenbo, Hu Ping. *Scripta Materialia*[J], 2009, 61(7): 690

18 Yan Yongjie, Huang Zhengren, Dong Shaoming *et al*. *Journal of the American Ceramic Society*[J], 2006, 89(11): 3589

19 Sarin P, Driemeyer P E, Haggerty R P *et al*. *Journal of the European Ceramic Society*[J], 2010, 30(11): 2375

20 Thompson M, Fahrenholtz W G, Hilmas G. *Journal of the American Ceramic Society*[J], 2011, 94(2): 429

21 Zamora V, Ortiz A L, Guiberteau F *et al*. *Journal of the European Ceramic Society*[J], 2012, 32(10): 2529

22 Fang Z Z, Wang H. *International Materials Reviews*[J], 2008, 53(6): 326

23 Guo S Q, Nishimura T, Kagawa Y *et al*. *Journal of the American Ceramic Society*[J], 2008, 91(9): 2848

24 Venkateswaran T, Basu B, Raju G B *et al*. *Journal of the European Ceramic Society*[J], 2006, 26(13): 2431

25 Zimmermann J W, Hilmas G E, Fahrenholtz W G. *Materials Chemistry and Physics*[J], 2008, 112(1): 140

26 Sciti D, Silvestroni L, Nygren M. *Journal of the European Ceramic Society*[J], 2008, 28(6): 1287

27 Garay J E. *Annual Review of Materials Research*[J], 2010, 40: 445

28 Xiong Y, Fu Z Y, Wang H. *Materials Science and Engineering B*[J], 2006, 128(1-3): 7

29 Zhang Xinghong, Xu Lin, Du Shanyi *et al*. *Scripta Materialia*[J], 2008, 59(1): 55

30 Hu Ping, Gui Kaixuan, Hong Wenhu *et al*. *Journal of the European Ceramic Society*[J], 2017, 37(6): 2317

31 Sha J J, Li J, Wang S H *et al*. *Materials & Design*[J], 2015, 75: 160

32 Hong Wenhu, Gui Kaixuan, Hu Ping *et al*. *Journal of Advanced Ceramics*[J], 2017, 6(2): 110

纳米 ZrB$_2$ 粉体放电等离子烧结制备 ZrB$_2$ 基超高温陶瓷

桂凯旋[1]，张庆达[1]，朱冬冬[2]，王　刚[1]

(1. 安徽工程大学，安徽 芜湖 241000)

(2. 衢州学院 浙江省空气动力装备技术重点实验室，浙江 衢州 324000)

摘　要：采用纳米 ZrB$_2$ 粉体研究了 ZrB$_2$ 基超高温陶瓷的放电等离子烧结行为。由于采用纳米粉体，单相 ZrB$_2$ 在 1550 ℃的低温下即发生快速的致密化烧结。ZrB$_2$-SiC 陶瓷经 1800 ℃放电等离子烧结后可实现完全致密化，并且材料的抗弯曲强度高达 1078±162 MPa。在 1700 ℃采用放电等离子烧结成功制备了 ZrB$_2$-SiC-C$_f$ 复合材料，材料断口表现出明显的纤维拔出现象，导致其具有高的断裂韧性值（6.04 MPa·m$^{1/2}$）和非脆性断裂的模式。同时，ZrB$_2$-SiC-C$_f$ 复合材料具有很高的临界热冲击温差（627 ℃），表明该材料具有优异的抗热冲击性能。

关键词：硼化锆；超高温陶瓷；放电等离子烧结；碳纤维

作者简介：桂凯旋，男，1989 年生，博士，安徽工程大学机械与汽车工程学院，安徽 芜湖 241000，电话：0553-2871252，E-mail: guikx@ahpu.edu.cn